

Multi-person 3D pose estimation from unlabelled data

Daniel Rodríguez-Criado¹, Pilar Bachiller², George Vogiatzis¹ and Luis J. Manso¹

Abstract—Its numerous applications make multi-human 3D pose estimation a remarkably impactful area of research. Nevertheless, assuming a multiple-view system composed of several regular RGB cameras, 3D multi-pose estimation presents several challenges. First of all, each person must be uniquely identified in the different views to separate the 2D information provided by the cameras. Secondly, the 3D pose estimation process from the multi-view 2D information of each person must be robust against noise and potential occlusions in the scenario. In this work, we address these two challenges with the help of deep learning. Specifically, we present a model based on Graph Neural Networks capable of predicting the cross-view correspondence of the people in the scenario along with a Multilayer Perceptron that takes the 2D points to yield the 3D poses of each person. These two models are trained in a self-supervised manner, thus avoiding the need for large datasets with 3D annotations.

Index Terms—3D multi-pose estimation, deep learning, graph neural networks, unlabelled dataset

I. INTRODUCTION

Human detection and pose modelling has a plethora of applications, including video surveillance [1], assisted living [2] and autonomous vehicles [3]. In addition to any direct application, it is also the basis of trajectory prediction, interaction detection, and gesture recognition. The number and relevance of applications make it extremely impactful. Extensive research effort has been made in the past with different technologies such as LiDAR technology [4], [5], RGB cameras [6] and RGBD cameras [7], [8].

This work aims at providing three-dimensional full-skeleton detection technology based on self-supervised learning satisfying the following conditions that make it useful in general environments:

- 1) it must work with multiple people;
- 2) 3-dimensional data must be provided for all joints;
- 3) RGB cameras must be the only sensors;
- 4) no labelled data should be required;
- 5) it must work with occluded body parts;
- 6) it must be easily replicable.

RGB-based multi-human and multi-view 3D pose estimation is usually done in three steps: a) detect humans and estimate their 2D poses on the images using, for example, a Convolutional Neural network (CNN); b) search for correspondences in the different views of the people provided by the cameras; and c) estimate 3D poses for each person

based on the image coordinates of their joints for the different views. This work presents a novel solution for the second and third steps. For the first stage, there are numerous pose detectors based on CNNs [9], [10] that perform with high accuracy and low processing time.

Regarding the second step, which consists in associating the 2D poses that correspond to the same person in the different images, most of the literature addresses the problem using heuristics based on appearance and geometry cues. Examples of this are the use of epipolar geometry to assign a cost to each pose detected [11] or the embedding of appearance features using a pre-trained model to provide affinity scores between bounding boxes [12]. The pictorial structure model to do multi-human tracking was extended in [13]. However, they assume to know the number of people in the scene, which is not realistic. Due to the variability of the number of views and people in the scene, we propose a model based on Graph Neural Networks (GNNs) to match people's views. The use of machine learning improves the stability against occlusions. Additionally, GNNs are order-invariant and can manage a variable number of inputs.

Traditionally the final part (3D pose estimation) has been done using triangulation or pictorial structure models. The main limitation of these classic approaches stems from the inability to predict the occluded parts. If one of the keypoints is occluded in most of the views, these methods are not capable of (accurately) estimating its position. To overcome these limitations, we propose a solution based on machine learning. We argue that an artificial neural network can learn to *hallucinate* the occluded parts of the body even if the information from most of the cameras is missing. This hypothesis is based on the intuition that the network should be able to exploit contextual information from the rest of the joints and the existing views, if any. For instance, a network could learn to implicitly internalise the proportions of the human body and its bilateral symmetry. Therefore, if the keypoint for the elbow cannot be seen from any camera, knowing the position of the wrist and the average proportions of a human forearm (or the length of the opposite forearm), the network could infer the position of the elbow. It is important to take into account that there is some degree of diversity in body types and sizes, but usually, there is not a significant difference in their proportions. It would be very challenging to efficiently embed these helpful biases in non-data-driven approaches.

A significant limitation of current data-driven solutions is the necessity of annotating the datasets to train the models in a supervised fashion. This task is often arduous and requires expensive tracking systems. To avoid the need for annotated

¹Daniel Rodríguez-Criado, George Vogiatzis and Luis J. Manso are with the College of Engineering and Physical Sciences, Aston University, B4 7ET Birmingham, UK {190229717, g.vogiatzis, l.manso}@aston.ac.uk

²Pilar Bachiller is with the Robotics and Artificial Vision Laboratory, University of Extremadura, Extremadura, Spain pilarb@unex.es

ground truth, we propose a solution using self-supervised learning. This way, the loss function that the model must optimise can be inferred from the input of the network. This process is explained in detail in section III-C.

In summary, the contributions of this paper are twofold:

- An elegant solution for the ambiguities problem when matching different 2D poses from several cameras using a GNN that allows having a variable number of people in the scenario.
- A data-driven model that infers the 3D keypoints of the detected humans using self-supervised learning by back projecting the 3D predictions into the cameras to calculate the loss function.

The next section reviews the current state of the art in 2D and 3D pose estimation. The proposed method is described in section III. Experimental results on a public dataset in comparison to other state of the art methods are presented in section IV. Finally, section V summarizes the main conclusions and achievements of our work.

II. RELATED WORK

This section will briefly review the leading literature on 3D Human Pose Estimation (HPE). Additionally, it covers the most popular 2D detectors since they are leveraged in many 3D estimation models. It is worth noting that we do not mention works using RGB-D sensors (with depth channel) since this paper focuses on RGB camera only, with the advantage of a considerable reduction in equipment cost.

2D human pose estimators yield image coordinates of human anatomical keypoints in an RGB image for every detected person. Recently, deep learning has achieved a breakthrough in these models obtaining a higher performance and accuracy than previous work based on probabilistic and hand-crafted features [14]. Most of these learning-based models [9], [15], [16], [17] rely on Convolutional Neural Networks. Among the vast amount of 2D pose estimators, OpenPose [10] is one of the most known within the community. OpenPose leverages the concept of part affinity fields for human parts association using a bottom-up approach. A similar approach is followed by OpenPifPaf [18] and trt-pose¹. Another 2D pose detector example is HRNet [19], which can maintain high-resolution representations through the detection process, obtaining more accuracy and spatial precision. One of the most popular datasets used for training and evaluating these 2D models is COCO [20], containing more than 100K annotated images.

In relation to the **3D pose estimation** problem, fueled by the outstanding advances in 2D estimations, many works have tried to utilize these models for lifting 3D poses from the 2D points [21]. Many of them retrieve 3D human poses from monocular views [22], [23], [24], though they suffer from the unavoidable ill-posed problem of having several potential 3D poses from a single 2D representation. **Multi-view images** can reduce this ambiguity significantly,

providing models more robust against occlusions and noise. However, multi-view HPE with **multiple people** introduces the challenge of matching each person’s keypoints among the images of the different cameras. Previous works have addressed this problem with algorithms based on appearance and geometric information [12], [25]. Thus, *Dong et al.* [12] create affinity matrices based on the appearance between two views and use them as input to their model to infer the correspondence matrix.

Once the cross-view ambiguities have been solved, there are several techniques to merge the information from the different views to extract the 3D pose. Most classical approaches rely on epipolar geometry by triangulating the 3D points from the 2D points [26], [25], [27]. Other works tackle the problem with prediction models based on **deep learning** and CNNs [6], [28]. For example, *Hanyue et al.* [6] discretize the 3D space in small cubes called voxels. Then, they project the 2D heatmaps detected from all the cameras into the 3D space and apply two 3D convolutional models. The first model yields detection proposals for each person and the second one estimates the positions of the joints for each detection. This methodology avoids establishing cross-view correspondence based on poor-quality 2D poses. Nevertheless, these models are camera-configuration specific and therefore require scenario-specific datasets with precise annotations. The number of these datasets is scarce mainly due to the costly equipment needed as well as the condition of a controlled environment to record the data. Some examples are the Human3.6M dataset [29] with more than 10K annotations from 1k images and the CMU Panoptic dataset [30] with 5.5 hours of video from different angles and 1.5 million of 3D annotated skeletons.

Due to the impact of avoiding 3D annotations (e.g. the variety and amount of data could be much larger), self or semi-supervised learning methods have been studied in many works [31], [23], [32], [27]. *Kocabas et al.* [27] present an approach related in spirit but different in methodology to the work at hand. They use self-supervised learning for 3D human pose estimation by calculating the loss using epipolar geometry from multiple cameras’ 2D pose estimations. However, they only provide the 3D pose for a single person in the scenario using a combination of two CNNs.

III. METHOD

The proposed system consists of a three-staged pipeline: a) a skeleton detector, b) a multi-view skeleton matching Graph Neural Network (GNN), and c) a pose estimation multilayer perceptron (MLP). Given that there are very efficient solutions for the first stage of the pipeline, no new alternative is proposed in this work. In fact, our system is independent of the skeleton detector used. The multi-view skeleton matching and the pose estimation network are contributions of this work. The code is available at https://github.com/gnns4hri/3D_multi_pose_estimator

¹Project URL: https://github.com/NVIDIA-AI-IOT/trt_pose

A. System calibration and skeleton detection

Our proposal is not limited to a number or configuration of cameras but requires the camera configuration to be the same during data gathering and the final inference for pose estimation. Thus, a previous step for using the approach presented in this paper is to select a fixed world frame of reference and calibrate the whole system of cameras to obtain their extrinsic and intrinsic parameters. These parameters are used during the training and inference phases of the two proposed neural networks, as described in sections III-B and III-C.

Assuming that the system has been calibrated, the next step is to detect the people in the environment in the different cameras. Each person has to be represented by a set of image positions corresponding to the keypoints of their skeleton. This information is provided by a skeleton detector. As aforementioned, our proposal is not limited to a specific detector and can be used with any of them regardless of the number of keypoints they provide for each skeleton. Such a number only determines the size of the input features of each network.

B. Skeleton matching

Once the skeletons are detected in the different views, a crucial stage is to identify the skeletons belonging to the same person. Our approach for this problem leverages GNNs to learn the correspondence between all the views of a person.

One of the main limitations of learning-based approaches using supervised learning is the generation of the dataset. For this particular problem, assuming that each sample of the dataset contains a set of skeletons per view, it would be necessary to manually label each pair of skeletons belonging to two different views as matching/not-matching. To avoid this arduous process, we propose gathering data of individual persons moving around the environment -one at a time- and then mixing the data of individual persons to generate samples with multiple moving people.

In order to prepare the input of the GNN, a graph with two types of nodes called *head* nodes and *edge* nodes, is generated. Specifically, *head* nodes are used to represent an individual view of a person and *edge* nodes to connect the views. The feature vectors of the nodes have $N_k * N_c * 10 + 2$ elements, with N_k and N_c being the number of keypoints and cameras, respectively. For each keypoint and camera, the corresponding slice of the feature vector contains the following information:

- A binary value indicating if the keypoint has been detected.
- The pixel coordinates if the keypoint is visible (2 zeros otherwise).
- A value within the range $[0, 1]$ indicating the certainty of the detection of the keypoint (zero if the keypoint is not visible)
- Six elements encoding the 3D line passing through the origin of the camera and the keypoint (image plane

coordinates) in the world frame of reference. The line is represented by a point and a direction vector.

The two additional elements of the feature vectors are two one-hot encoding features that encode the node type (*head* or *edge*). For *edge* nodes all the features are set to 0 except the one representing the corresponding type of node. For *head* nodes, beside the node type, only the features corresponding to the associated view are filled and the remaining ones are set to 0.

The GNN is trained to generate a single output for each node, representing a person matching score in the range $[0, 1]$. Only *edge* nodes are considered for that. During the generation of the dataset, a score of 0 or 1 has to be assigned to the *edge* nodes depending on whether they are connecting a pair of *head* nodes belonging to different people or to the same person. As was mentioned previously, to avoid manual labelling, we use data obtained from individual persons moving around, so all views certainly match. These data are used to generate separated graphs for each person for which all the *edge* nodes are assigned a maximum score value (see figures 1a and 1b). Then, the graphs of individual persons are combined through edge nodes with 0 score, as shown in figure 1c and the GNN can be trained in a supervised fashion without the need of labels. The number of graphs to be combined is arbitrary. It is randomly chosen for each sample of the dataset considering a minimum of 1 and a maximum of 10 people in the scene.

C. 3D Pose estimation

Having identified the different views of each person, an MLP is in charge of estimating the 3D coordinates of the keypoints for each of them. Thus, the proposed system uses one MLP instance per person.

The total input features of the model are the concatenation of 14 features per keypoint and camera. Therefore, if the skeleton detector model can detect 25 keypoints coordinates and the system uses 4 cameras, the dimension of the input feature vector would be $14 \times 4 \times 25$ or 1400 features in total. The 14 features per keypoint correspond to the 10 features described in the previous section for skeleton matching plus four additional features related to an initial estimation of the 3D. Specifically, if a keypoint of a person is detected by 2 or more cameras, its 3D coordinates are reconstructed by triangulation for every pair of cameras and an initial estimation is computed as the centroid of the obtained 3D points. This estimation is included as input using three of the four new features. The last feature is used to indicate the availability of the estimated 3D. It is set to 1 if there is more than one view of the keypoint and to 0 otherwise.

Using the aforementioned information per keypoint and camera, the network estimates the 3D positions of the keypoints in the world frame of reference, yielding x , y and z for each of them. Thus, assuming that the network predicts the position of 25 different keypoints, the output vector dimension is $3 \times 25 = 75$.

Regarding the training process, as explained in the introduction, it follows a self-supervised learning approach. In

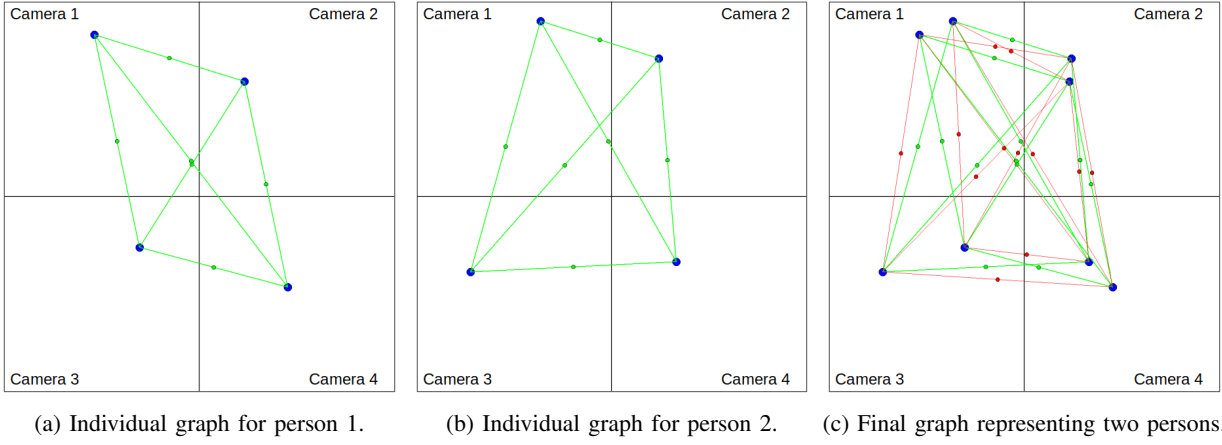


Fig. 1: Generation of a sample of the dataset. Graphs of individual persons are generated first assigning a score of 1 to the *edge* nodes connecting the views (green nodes and lines). Then a final graph is generated from the individual ones adding *edge* nodes with a score of 0 (red nodes and lines).

this way, there is no need to use a ground truth to compare the output, since the loss function can be inferred from the input data. However, calculating this loss is not trivial in this case since the network infers 3D poses from 2D positions. Our approach to solve this problem is to back-project the 3D coordinates of the keypoints predicted by the network into each image. The translation between world and image coordinates is done by using the transformation matrices obtained during the calibration process and the intrinsic properties of each camera. Using the back-projected coordinates and the coordinates yielded by the skeleton detector, an error measurement of the estimation of the network is obtained. This error is used to define the loss function that the network must minimise. More formally, assuming that the output of the network o is represented as a vector of 3D positions corresponding to the estimation of the person's keypoints coordinates:

$$o := (o_0, o_1, \dots, o_{N_k-1}) \quad (1)$$

with N_k the number of keypoints, and being T_c the projection matrix of the camera c , a vector p_c of image projected positions (p_{ci}) can be obtained for each camera as follows:

$$p_{ci} = T_c * o_i \quad \forall i \in [0, N_k) \quad (2)$$

Using p_c and the set of detected keypoints ($S_c = \{s_{ck}\}$) for each camera c , the projection error e is computed as

$$e = \sum_{c=0}^{N_c-1} \sum_{s_{ck} \in S_c} d(p_{ck}, s_{ck}) \quad (3)$$

being $d(\cdot)$ the distance between the projected and detected points. In particular, we use the Manhattan distance for d .

Applying equation 3 to each sample of a data batch B of size BS , the final loss is calculated using the mean squared error:

$$\mathcal{L} = \sum_{b \in B} e_b^2 / BS \quad (4)$$

being e_b the result of equation 3 for the sample b .

Figure 2 depicts this process assuming 25 keypoints and 4 cameras.

IV. EXPERIMENTAL RESULTS

Our 3D multi-human pose estimation system has been tested using the CMU Panoptic Studio dataset [30] through a set of experiments that are presented in this section.

To perform these experiments, the two neural models were trained using ten sequences of CMU Panoptic for five different views. We use the same sequences and views as VoxelPose [6] for comparison purposes. Similarly, the four sequences used for testing VoxelPose were applied in our experiments. The data with the 2D skeletons' information were obtained using the backbone model provided in the VoxelPose project. Using this model, the 2D coordinates of the humans' keypoints were detected from the images. Nevertheless, our training strategy requires that each sample of the data includes the information of only one person, so it was necessary to organize the detection results to provide individual human data. To this end, the skeletons of the different views belonging to the same human were identified using the ground truth of the Panoptic sequences and grouped to obtain individual samples for each human. In addition, we applied data augmentation to extend the amount of data used for training and the variety of situations. Specifically, for each original sample of the dataset, which we refer to as seed samples, several samples were generated removing the information of some of the views. These new data are used as normal input of the two networks, but, in the case of the pose estimation network, for each generated sample, the data of its seed sample is used in the computation of the loss (equation 4). This way, the network can learn to estimate the positions of occluded keypoints.

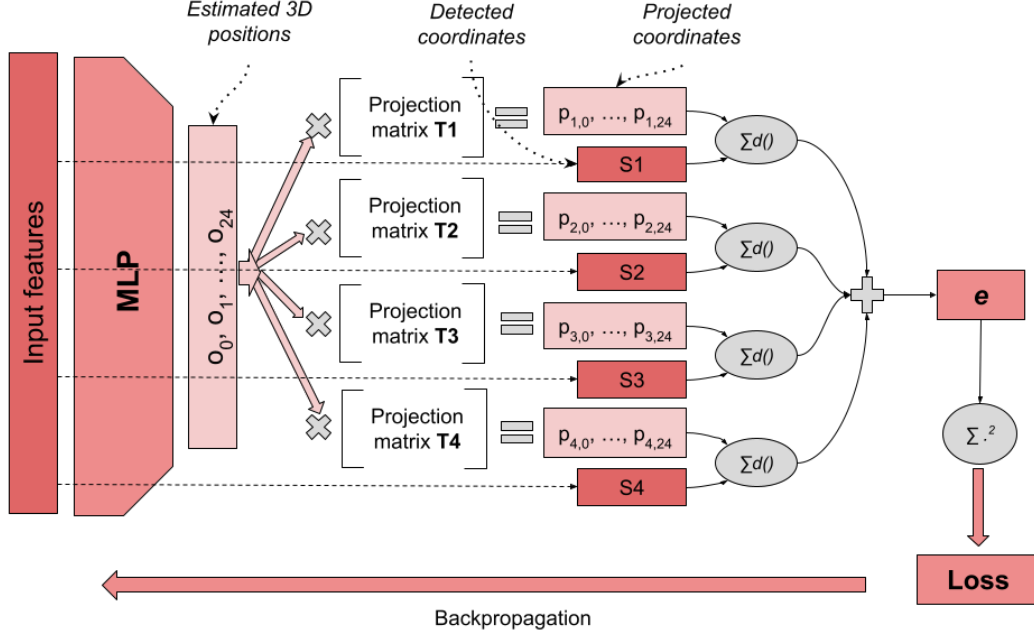


Fig. 2: Loss computation during the training phase of the 3D pose estimation network.

Regarding the architecture of the two neural networks, we use a Graph Attention Network (GAT) with 4 hidden layers for skeleton matching. The hidden layers are composed of [40, 40, 40, 30] hidden units and [10, 10, 8, 5] attention heads. LeakyReLU and Sigmoid are used as activation functions of the hidden and output layers, respectively. The MLP for pose estimation has 7 hidden layers of [3072, 3072, 2048, 2048, 1024, 1024, 1024] hidden units, using LeakyReLU for the activation of the hidden layers and linear activation in the output layer.

The two models were trained and evaluated using the test sequences of Panoptic through the following metrics:

- Recall: percentage of correctly estimated poses in relation to the total number of ground truth poses for a given distance threshold. Specifically, for a distance threshold th , an estimated pose is considered correct if the mean distance per keypoint to the ground truth is smaller than th .
- Precision: percentage of correctly estimated poses in relation to the total number of detected poses for a given distance threshold.
- Average precision (AP): average precision according to the precision-recall curve for a given distance threshold (as computed in [6]).
- MPJPE (mean per joint precision): mean distance per keypoint between detected and ground truth poses.
- Time for persons' proposals (t_{pp}): mean time required for generating persons' proposals. In our approach, this

time corresponds to the skeleton matching stage.

- Time for 3D pose estimation (t_{3Dg}): mean time required for estimating the 3D poses.
- Time for 3D pose estimation per human (t_{3Di}): mean time required for estimating the 3D pose of one person.

The results of these metrics for our proposal are shown in table I. We consider distance thresholds from 25mm to 150mm, with steps of 25mm. As can be observed, the MPJPE is 29.79mm, so the values for recall, precision and AP for the smallest distance threshold are very low. Nevertheless, from a distance threshold of 50mm, the accuracy results are reasonably good. Furthermore, recall and precision have very similar values, indicating that the number of people detected matches the actual number of people for the vast majority of samples in the test sequences, which shows the robustness of the skeleton matching model. Regarding the computational complexity, the mean time employed by our system to estimate all the 3D poses from the detected image keypoints is 77.02ms. In particular, the skeleton matching stage takes 40.89ms on average. The time spent in this stage is dependent on the number of views and people in the scene since the computational cost of the generation of the graph and analysis of the network output is directly related to the complexity of the graph. The 3D pose estimation stage takes 10.62ms per person, with an average of 36.13ms for each sample of the test sequences.

To assess the performance of our proposal, the results of our pose estimation model were compared with the 3D poses

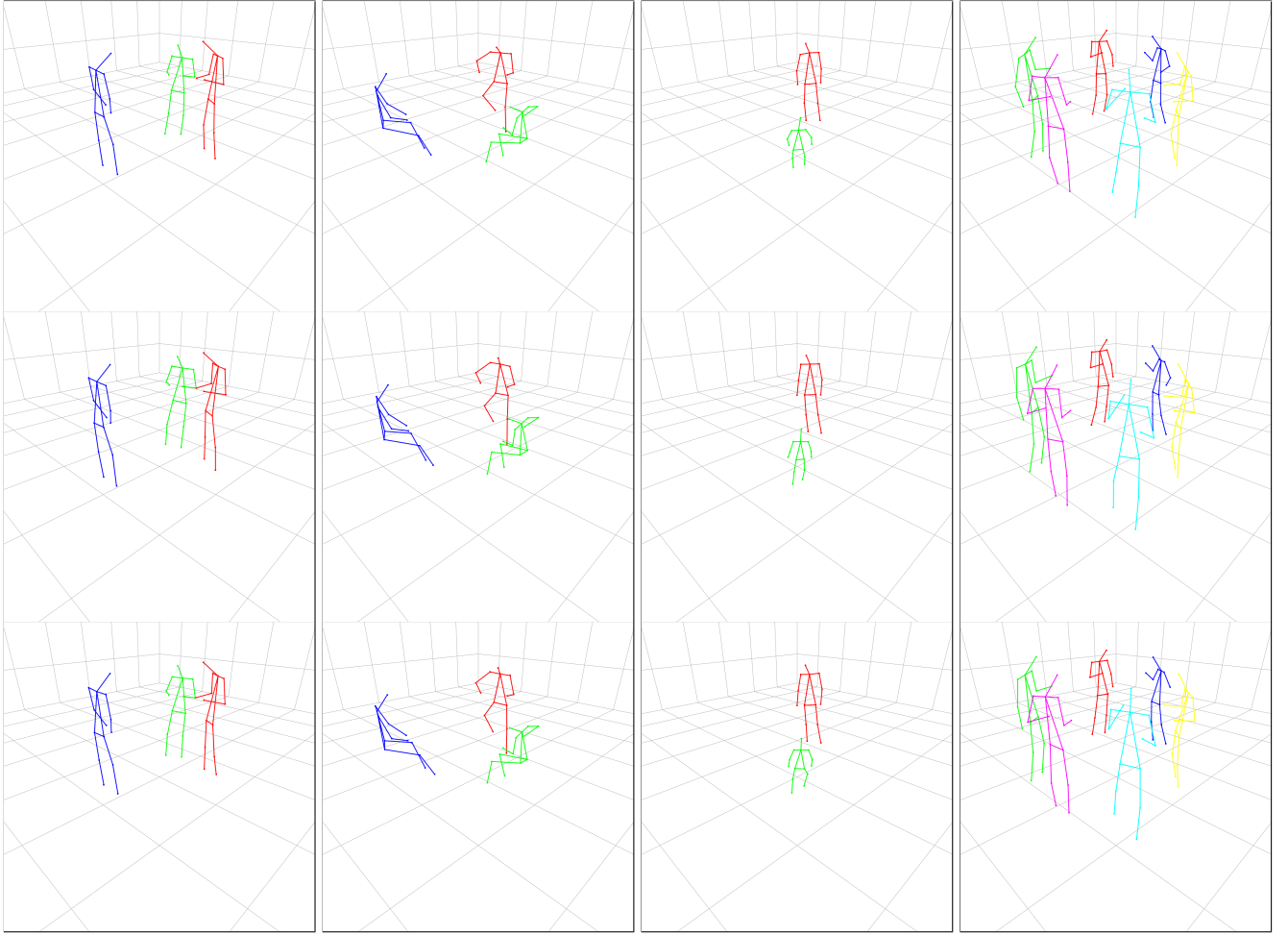


Fig. 3: Pose estimation results for 4 samples of the test sequences using our model (first row) and triangulation (third row) in comparison with the ground truth (second row). Triangulation provides complete poses in the 4 samples.

TABLE I: New table: Accuracy and time metrics for our proposal

Threshold/mm	25	50	75	100	125	150
Recall/%	36.72	96.33	98.26	99.20	99.43	99.53
Precision/%	36.75	96.41	98.34	99.28	99.51	99.61
AP/%	18.66	93.82	97.13	98.71	99.12	99.27
MPJPE/mm	29.79					
t_{pp}/ms	40.89					
t_{3Dg}/ms	36.13					
t_{3Di}/ms	10.62					

obtained by triangulation. With this aim, for each pair of views of a person identified by the skeleton matching model, the 3D position of each visible keypoint was estimated by triangulating the 3D of its 2D coordinates. If more than one estimation was obtained (*i.e.*, the keypoint is visible from more than 2 cameras), the final 3D position for the keypoint was computed as the average of the individual estimations. Using this procedure, we obtained the results of table II. As shown in this table, the MPJPE is lower than that obtained by the pose estimation model, although its computation only considers the keypoints for which triangulation can

be applied, that is, the keypoints visible from two or more cameras. In fact, the results for recall, precision and AP are worst than those shown in table I, except for the first distance threshold. The reason is that triangulation does not always provide complete pose estimations. Figures 3 and 4 show some examples of complete and incomplete results using triangulation. From top to bottom, the three rows in these figures correspond to our pose estimation model, the ground truth and pose estimation by triangulation. Specifically, figure 3 presents some samples for which all the keypoints of every person in the scene can be estimated by triangulation. For these samples, the estimated poses provided by both, our model and the triangulation technique, are very close to the ground truth poses. On the other hand, in figure 4, some poses can not be fully determined by triangulation because there are keypoints that are not visible from two or more cameras. In these situations, our model provides complete estimates for all poses, presenting minimal differences with the ground truth.

To complete the experimental analysis of our proposal, VoxelPose was trained using the same ten training Panoptic sequences. Results on the metrics for the four test sequences

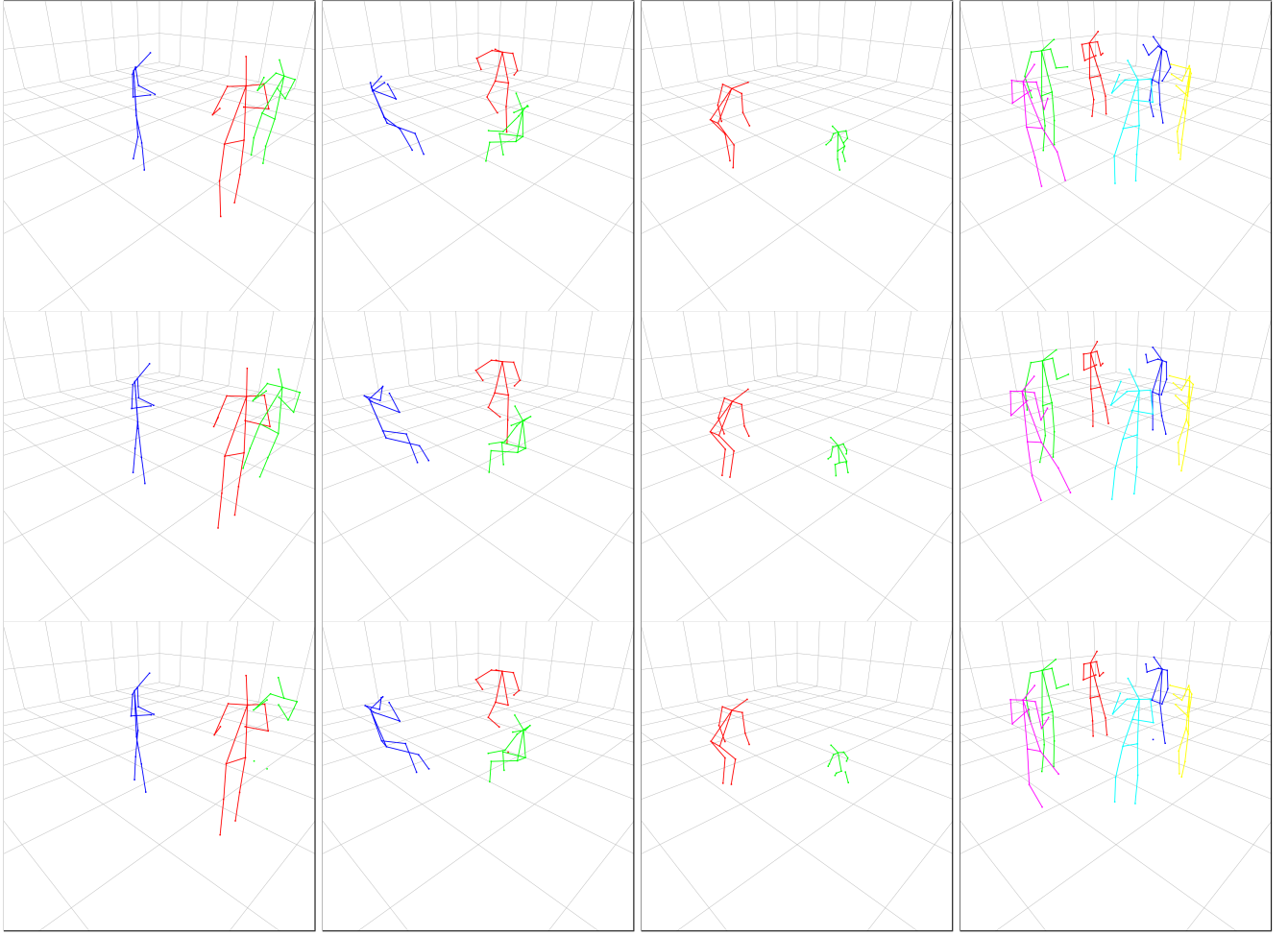


Fig. 4: Pose estimation results for 4 samples of the test sequences using our model (first row) and triangulation (third row) in comparison with the ground truth (second row). In these samples, triangulation can not provide complete poses due to an insufficient number of views for some keypoints.

TABLE II: Accuracy and time metrics for triangulation

Threshold/mm	25	50	75	100	125	150
Recall/%	69.84	87.89	87.98	87.99	87.99	87.99
Precision/%	69.85	87.91	88.00	88.01	88.01	88.01
AP/%	55.52	80.90	81.07	81.08	81.08	81.08
MPJPE/mm	23.54					
t_{pp}/ms	40.23					
t_{3Dg}/ms	10.17					
t_{3Di}/ms	3.00					

are presented in table III. In general, the accuracy metrics for VoxelPose show better results than our proposal, with a notable difference for the lower distance threshold. Nevertheless, the differences between both approaches become less significant as the distance threshold increases. In addition, the *Recall/Precision* ratio is smaller than ours, which indicates greater divergences between the number of people detected and the actual number. In relation to the time metrics, the mean time required for the whole estimation process is 305.91ms, which is almost 4 times the time employed by our proposal, although the data in table I does not include the

time for skeleton detection. That time can vary depending on the specific detector and the available hardware, but there exist very efficient solutions. For instance, trt-pose can perform at 251 FPS on Jetson Xavier, as reported in their software project (https://github.com/NVIDIA-AI-IOT/trt_pose). In addition, the skeleton detection for all the views could be run in parallel, making the timing independent of the number of views. Thus, assuming that skeleton can be detected at 30 FPS, **our proposal still runs 3 times faster** than VoxelPose.

TABLE III: Accuracy and time metrics for VoxelPose

Threshold/mm	25	50	75	100	125	150
Recall/%	89.55	98.29	98.95	99.17	99.24	99.26
Precision/%	90.07	98.86	99.52	99.74	99.81	99.83
AP/%	84.95	98.17	98.92	99.15	99.22	99.24
MPJPE/mm	17.97					
t_{pp}/ms	135.92					
t_{3Dg}/ms	169.99					
t_{3Di}/ms	50.53					

Besides the aforementioned benefits regarding the real-

time execution property of our 3D multi-pose estimator, we consider that our proposal provides a more general solution to the problem than the existing alternatives. The fact that **no ground truth is required** to train the two models makes our proposal easily replicable, regardless of the space organization and extension.

V. CONCLUSIONS

Multi-person 3D pose estimation is an important research field with multiple applications, including but not limited to human-robot interaction. Deep learning is a powerful tool for that. Nevertheless, conventional deep learning solutions require a large amount of labelled data. To overcome this limitation, this work proposes a deep learning-based approach for the 3D multi-pose estimation problem that uses completely unannotated data. Specifically, we propose a GNN to identify the views of the different people in the scene and an MLP to estimate the complete 3D pose of each person. The unique requirement for the training of each network is that each element in the dataset corresponds to an individual person. Both networks use information that can be directly obtained from the RGB images, so our approach only requires regular RGB cameras.

Experimental results using the CMU Panoptic dataset show a mean per joint precision error of 29.79mm, which can be considered more than acceptable for many applications. In addition, the *recall/precision* ratio is very close to unity, demonstrating the robustness of our skeleton matching model. The comparison to VoxelPose shows higher accuracy values than those of our proposal, although the differences are less remarkable for distance thresholds greater than the aforementioned MPJPE (25mm). Furthermore, the computational complexity of our system is significantly lower than VoxelPose, making it an effective solution for real-time applications.

Looking into the future, we would like to improve the accuracy of our estimator model by refining the training with hyperparameter tuning. Additionally, we have thought about two projects to extend the present work: train the system with cameras mounted on a mobile robot that can be very useful for robot navigation applications; design a model capable of learning the intrinsics and extrinsics of the cameras to generalize over different scenarios. With this last project, the model would be scenario agnostic and the user would only need to mount the cameras and run the system without any training.

REFERENCES

- [1] X. Wang, "Intelligent multi-camera video surveillance: A review," *Pattern Recognit. Lett.*, vol. 34, pp. 3–19, 2013.
- [2] F. Cardinaux, D. Bhowmik, C. Abhayaratne, and M. Hawley, "Video based technology for ambient assisted living: A review of the literature," *JAISE*, vol. 3, pp. 253–269, 05 2011.
- [3] D. Gerónimo, A. M. López, A. D. Sappa, and T. Graf, "Survey of pedestrian detection for advanced driver assistance systems," *IEEE Transactions on Pattern Analysis and Machine Intelligence*, vol. 32, no. 7, pp. 1239–1258, 2010.
- [4] Z. Yan, T. Duckett, and N. Bellotto, "Online learning for human classification in 3d lidar-based tracking," in *2017 IEEE/RSJ International Conference on Intelligent Robots and Systems (IROS)*, 2017, pp. 864–871.
- [5] T. Taipalus and J. Ahtiainen, "Human detection and tracking with knee-high mobile 2d lidar," in *2011 IEEE International Conference on Robotics and Biomimetics*, 2011, pp. 1672–1677.
- [6] H. Tu, C. Wang, and W. Zeng, "Voxelpose: Towards multi-camera 3d human pose estimation in wild environment," in *European Conference on Computer Vision*. Springer, 2020, pp. 197–212.
- [7] M. Camplani, A. Paiement, M. Mirmehdi, D. Damen, S. Hannuna, T. Burghardt, and L. Tao, "Multiple human tracking in RGB-depth data: A survey," *IET Computer Vision*, vol. 11, no. 4, pp. 265–285, 2017.
- [8] J. Zhang, W. Li, P. O. Ogunbona, P. Wang, and C. Tang, "RGB-D-based action recognition datasets: A survey," *Pattern Recognition*, vol. 60, pp. 86–105, 2016. [Online]. Available: <https://www.sciencedirect.com/science/article/pii/S0031320316301029>
- [9] W. Abdulla, "Mask R-CNN for object detection and instance segmentation on Keras and TensorFlow," https://github.com/matterport/Mask_RCNN, 2017, gitHub repository.
- [10] Z. Cao, G. Hidalgo Martinez, T. Simon, S. Wei, and Y. A. Sheikh, "Openpose: Realtime multi-person 2d pose estimation using part affinity fields," *IEEE Transactions on Pattern Analysis and Machine Intelligence*, 2019.
- [11] L. Bridgeman, M. Volino, J.-Y. Guillemaut, and A. Hilton, "Multi-person 3d pose estimation and tracking in sports," in *2019 IEEE/CVF Conference on Computer Vision and Pattern Recognition Workshops (CVPRW)*, 2019, pp. 2487–2496.
- [12] J. Dong, Q. Fang, W. Jiang, Y. Yang, Q. Huang, H. Bao, and X. Zhou, "Fast and robust multi-person 3d pose estimation and tracking from multiple views," *IEEE Transactions on Pattern Analysis and Machine Intelligence*, 2021.
- [13] V. Belagiannis, S. Amin, M. Andriluka, B. Schiele, N. Navab, and S. Ilic, "3d pictorial structures for multiple human pose estimation," in *2014 IEEE Conference on Computer Vision and Pattern Recognition*, 2014, pp. 1669–1676.
- [14] H. Chen, R. Feng, S. Wu, H. Xu, and F. Zhou, "2D Human Pose Estimation: A Survey," pp. 1–26.
- [15] S. Kreiss, L. Bertoni, and A. Alahi, "PifPaf: Composite fields for human pose estimation," *Proceedings of the IEEE Computer Society Conference on Computer Vision and Pattern Recognition*, vol. 2019-June, pp. 11 969–11 978, 2019.
- [16] A. Jain, J. Tompson, M. Andriluka, G. W. Taylor, and C. Bregler, "Learning human pose estimation features with convolutional networks," *2nd International Conference on Learning Representations, ICLR 2014 - Conference Track Proceedings*, pp. 1–11, 2014.
- [17] J. Tompson, A. Jain, Y. LeCun, and C. Bregler, "Joint training of a convolutional network and a graphical model for human pose estimation," *Advances in Neural Information Processing Systems*, vol. 2, no. January, pp. 1799–1807, 2014.
- [18] S. Kreiss, L. Bertoni, and A. Alahi, "Openpifpaf: Composite fields for semantic keypoint detection and spatio-temporal association," *IEEE Transactions on Intelligent Transportation Systems*, 2021.
- [19] K. Sun, B. Xiao, D. Liu, and J. Wang, "Deep high-resolution representation learning for human pose estimation," *Proceedings of the IEEE Computer Society Conference on Computer Vision and Pattern Recognition*, vol. 2019-June, pp. 5686–5696, 2019.
- [20] T. Y. Lin, M. Maire, S. Belongie, J. Hays, P. Perona, D. Ramanan, P. Dollár, and C. L. Zitnick, "Microsoft COCO: Common objects in context," *Lecture Notes in Computer Science (including subseries Lecture Notes in Artificial Intelligence and Lecture Notes in Bioinformatics)*, vol. 8693 LNCS, no. PART 5, pp. 740–755, 2014.
- [21] J. Wang, S. Tan, X. Zhen, S. Xu, F. Zheng, Z. He, and L. Shao, "Deep 3D human pose estimation: A review," *Computer Vision and Image Understanding*, vol. 210, no. August 2020, p. 103225, 2021. [Online]. Available: <https://doi.org/10.1016/j.cviu.2021.103225>
- [22] S. Li and A. B. Chan, "3d human pose estimation from monocular images with deep convolutional neural network," in *Asian Conference on Computer Vision*. Springer, 2014, pp. 332–347.
- [23] G. Pavlakos, X. Zhou, K. G. Derpanis, and K. Daniilidis, "Coarse-to-fine volumetric prediction for single-image 3D human pose," *Proceedings - 30th IEEE Conference on Computer Vision and Pattern Recognition, CVPR 2017*, vol. 2017-January, pp. 1263–1272, 2017.
- [24] F. Moreno-Noguer, "3D human pose estimation from a single image via distance matrix regression," *Proceedings - 30th IEEE Conference on Computer Vision and Pattern Recognition, CVPR 2017*, vol. 2017-January, pp. 1561–1570, 2017.

- [25] V. Belagiannis, S. Amin, M. Andriluka, B. Schiele, N. Navab, and S. Ilic, "3D Pictorial Structures Revisited: Multiple Human Pose Estimation," *IEEE Transactions on Pattern Analysis and Machine Intelligence*, vol. 38, no. 10, pp. 1929–1942, 2016.
- [26] S. Amin, M. Andriluka, M. Rohrbach, and B. Schiele, "Multi-view pictorial structures for 3d human pose estimation," in *Bmvc*, vol. 1, no. 2, 2013.
- [27] M. Kocabas, S. Karagoz, and E. Akbas, "Self-supervised learning of 3D human pose using multi-view geometry," *Proceedings of the IEEE Computer Society Conference on Computer Vision and Pattern Recognition*, vol. 2019-June, pp. 1077–1086, 2019.
- [28] D. Rodriguez-Criado, P. Bachiller, P. Bustos, G. Vogiatzis, and L. J. Manso, "Multi-camera torso pose estimation using graph neural networks," in *2020 29th IEEE International Conference on Robot and Human Interactive Communication (RO-MAN)*. IEEE, 2020, pp. 827–832.
- [29] C. Ionescu, D. Papava, V. Olaru, and C. Sminchisescu, "Human3.6m: Large scale datasets and predictive methods for 3d human sensing in natural environments," *IEEE Transactions on Pattern Analysis and Machine Intelligence*, vol. 36, no. 7, pp. 1325–1339, 7 2014.
- [30] H. Joo, H. Liu, L. Tan, L. Gui, B. C. Nabbe, I. A. Matthews, T. Kanade, S. Nobuhara, and Y. Sheikh, "Panoptic studio: A massively multiview system for social motion capture," in *2015 IEEE International Conference on Computer Vision, ICCV 2015, Santiago, Chile, December 7-13, 2015*. IEEE Computer Society, 2015, pp. 3334–3342.
- [31] D. Drover, M. V. Rohith, C. H. Chen, A. Agrawal, A. Tyagi, and C. P. Huynh, "Can 3D pose be learned from 2D projections alone?" *Lecture Notes in Computer Science (including subseries Lecture Notes in Artificial Intelligence and Lecture Notes in Bioinformatics)*, vol. 11132 LNCS, pp. 78–94, 2019.
- [32] H. Rhodin, F. Meyer, J. Spörri, E. Muller, V. Constantin, P. Fua, I. Katircioglu, and M. Salzmann, "Learning Monocular 3D Human Pose Estimation from Multi-view Images," *Proceedings of the IEEE Computer Society Conference on Computer Vision and Pattern Recognition*, pp. 8437–8446, 2018.